doi: 10.1111/j.1365-3121.2005.00605.x

Denudation of the Côte d'Ivoire-Ghana transform continental margin from apatite fission tracks

Florence Bigot-Cormier,[1] Christophe Basile,[2] Gérard Poupeau,[3] Jean-Pierre Bouillin[2] and Erika Labrin[2]
[1]*Géosciences Azur, UMR 6526, Faculté des Sciences, Parc Valrose, 06108 Nice cedex 02;* [2]*LGCA, CNRS-UMR 5025, OSUG, Université Joseph Fourier, Grenoble;* [3]*CRPAA-Maison de l'Archéologie, UMR 5060 of CNRS, Université Bordeaux III, 33607 Pessac, France*

ABSTRACT

Apatite fission track analysis of samples from the shoulder (marginal ridge) of the Côte d'Ivoire-Ghana transform continental margin reveal a cooling of the margin between 85 and 65 Ma for the central and eastern parts of the ridge. All samples were heated *in situ* during sedimentary burial with a temperature >120 °C, except for two samples located in the eastern part which were heated between 105 and 120 °C. For the first time, age/depth diagram along a transform margin shows a shape involving erosion starting at the bottom of the continental slope, then stepping backwards towards the edge of the slope. This retrogressive erosion can result from the deepening of the lithospheric plate sliding along the transform margin, from thick continental crust to thin continental crust, and finally to oceanic crust. This process could be at the origin of the shoulder uplift by flexural response to the important crustal discharge (>2 km).

Terra Nova, 17, 189–195, 2005

Introduction and geological setting

North of the Gulf of Guinea, the Côte d'Ivoire-Ghana (CIG) ridge is 25 km wide (Fig. 1), 130 km long structure that strikes WSW–ENE from the Romanche Fracture Zone to the Ghanaian shelf (Fig. 2A). It represents the southern edge of the Deep Ivorian Basin (DIB). The bathymetric ridge overlays a strongly asymmetric structural ridge, standing above the DIB by about 1300 m, while its southern slope dominates the ocean floor by a >4000 m scarp (Fig. 1; Basile *et al*., 1993).

According to Mascle and Blarez (1987) and Basile *et al*. (1993, 1998), three stages can be distinguished in the tectonic evolution of the CIG transform margin:

1 Early Cretaceous (Aptian or older) intracontinental rifting and transform faulting. The rifting ends with the formation of an oceanic crust west of the DIB during Albian-Cenomanian times (105–95 Ma). During this first stage, lacustrine sedimentation began in half-grabens delimited by N–S and NE–SW normal faults, and was overlaid by marine sediments prograding from the south, suggesting that the sediments came from the Brazilian shelf (Blarez and Mascle, 1988; Lamarche *et al*., 1997). These deformed sediments outcrop all along the southern slope of the CIG marginal ridge, and lie below an unconformity along the northern slope (Fig. 1). Biostratigraphy did not provide ages younger than late Albian in this sedimentary unit.
2 Turonian continent-ocean active transform margin, resulting from the equatorial Atlantic onset of seafloor spreading *c*. 90 Ma (Mascle *et al*., 1988). Contemporaneous sediments are known only in the DIB, and onlap the northern slope of the marginal ridge (Fig. 1).
3 After the passing of the oceanic accretion axis south of the transform margin during the Santonian (85–80 Ma), the continent-ocean transform margin was passive. Younger sediments filled horizontally the DIB (Fig. 1). The present day continental slope exhibits three distinct morphostructural units (Basile *et al*., 1993; Lamarche *et al*., 1997; Sage *et al*., 1997, 2000) (Fig. 2A): (i) the central part (very steep and about linear continental slope) that coincides with the topographically high CIG ridge; (ii) the westernmost part (ridge termination) where the continental slope becomes less steep and changes from ENE–WSW to E–W strike; (iii) the easternmost part, which belongs to the Ghanaian continental slope, that does not exhibit any marginal ridge, and where canyons cutting the slope are fed directly from the Ghanaian shelf.

Since Todd and Keen (1989), the formation of transform marginal ridges has often been explained by heating (and associated uplift) of the continental lithosphere by the accretion of oceanic crust against the transform margin. More recently, based on numerical modelization and apatite fission tracks (FT) data from Oceanic Drilling Program (ODP) Leg 159 samples, Clift and Lorenzo (1999) explained the uplift by a combination of thermal uplift and tectonic denudation associated to transtensional faulting. Nevertheless, as the CIG ridge appeared as an uplifted area since the late Albian (Basile *et al*., 1998), a long time before the oceanic accretion against the transform margin, this thermal model does not seem suitable.

Along the CIG ridge, thermal aspects of the evolution of the transform marginal ridge were first investigated through apatite FT in six samples from the Equanaute cruise (Bouillin *et al*., 1994, 1997, 1998) and additional samples from ODP Leg 159 (Bouillin *et al*., 1998; Clift *et al*., 1998), which provided only one vertical section and sparse information along the margin. While the ODP core samples came from drill holes atop or near to the top of the CIG ridge, 153 Equanaute samples were taken *in situ* along 14 submarine profiles, dedicated to the sedimentary, stratigraphic and structural study of

Correspondence: Florence Bigot-Cormier. Tel.: +33 4 92 07 68 15; fax: +33 4 92 07 68 16; e-mail: florence.bigot@unice.fr

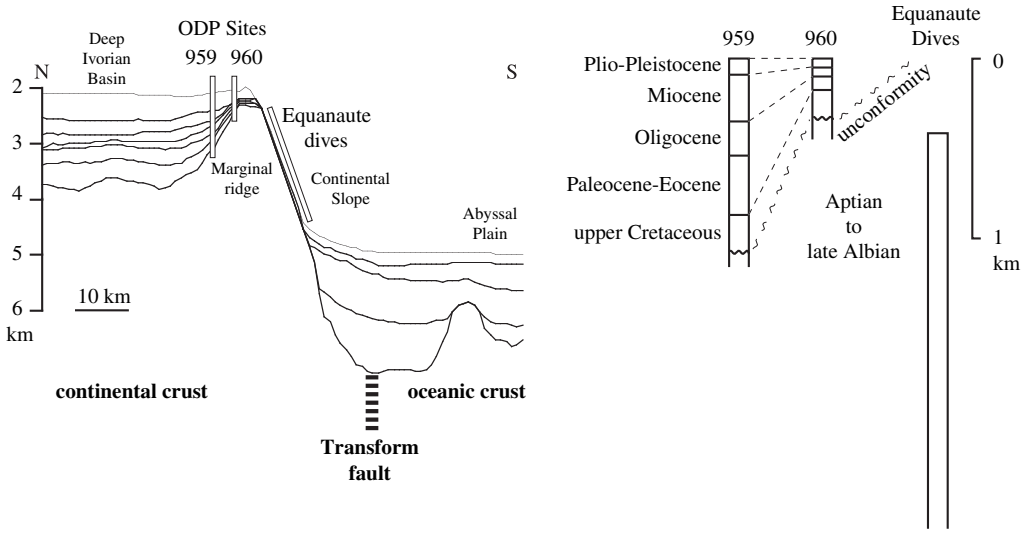

Fig. 1 N–S section of the CIG transform continental margin with main sedimentary reflectors (vertical exaggeration 10, modified from Mascle and Basile, 1998), and stratigraphic relationships between three sections across the transform margin [ODP sites 959 and 960 (modified from Mascle *et al.*, 1996), and Equanaute dives (Mascle *et al.*, 1998)].

the 2.5 km high outcrops along the steep continental slope (Mascle *et al.*, 1998). We integrate in this study the six previously published apatite FT analysis and 11 additional samples to investigate and quantify for the first time the spatial (i.e. both horizontally and through several vertical sections) and temporal evolution of heating and denudation along the uplifted shoulder of the transform continental margin. We first discuss the thermal history, then the vertical motion of the CIG ridge in relation with the crossing of the oceanic accretion axis.

Sampling strategy and experimental procedures

The 17 analysed Equanaute samples come from the Lower Cretaceous formation (middle to latest Albian: Klingebiel, 1976; Mascle *et al.*, 1998) between 4800 and 2200 m depth, all along the marginal ridge, and as far as possible at various depths along the same diving profiles (EN02, EN04, EN07, EN08; Fig. 2 and Table 1).

Apatite FT datations were realized with the external detector method (Hurford and Green, 1983; Hurford and Carter, 1991) using the zeta technique (Fleischer and Hart, 1972).

Irradiations were performed in the Orphée nuclear reactor of the Centre d'Etudes Nucléaires of Saclay (France). Each age was calculated with the central age method (Galbraith and Laslett, 1993), except for the previously studied samples (Bouillin *et al.*, 1997) (pooled ages; Galbraith, 1981; Green, 1981).

Confined track lengths were measured in 13 apatite samples, including six previously studied by Bouillin *et al.* (1997).

New results

Analytical data are presented in Table 1 and sample locations and their FT ages in Fig. 2. In all samples except the two easternmost ones, there is only one age population among the crystals dated, as suggested by the chi-squared test of Galbraith (1981) and Green (1981) and by the standard deviation obtained for central ages (Galbraith and Laslett, 1993). The corresponding confined track lengths are consistently longer than 14 μm with standard deviation from 1.1 (EN09-9) to 1.5 μm (EN07-11) (Table 1), which testify that the CIG margin cooled rapidly. Figure 2B gives two typical examples of radial plots for samples of this group. These ages range from 92 to 64 Ma, and are all younger than the stratigraphic age of the sediments. There is no clear trend of ages horizontally along the transform margin (Fig. 2A); vertically it appears that the older ages come from the deeper samples, while the younger ages come from the shallower samples.

In the easternmost samples EN02-7 and EN02-8, chi-squared probabilities $< 5\%$ indicate that more than one age population is present among the dated apatites (Table 1). In sample EN02-7, the Galbraith (1981) method discriminates two age populations, aged respectively 85.4 ± 7.3 and 147.4 ± 14.9 Ma (Fig. 2B). In EN02-8, dated with the same number of apatite as EN02-7, the large dispersion of individual grains FT ages do not allow one to identify age populations. However, the five youngest apatite grains define a population 75.6 ± 7.5 Ma (Table 1). In these two samples, several grains have FT ages older than their early Cretaceous sedimentation age (Mascle *et al.*, 1996), hence they were not heated enough *in situ* to lose their pre-detrital tracks. The individual grains age distributions in these two samples and confined track lengths in EN02-07 suggest that (i) this part of the CIG was only mildly affected by post-depositional heating and that (ii) apatites with various chemical compositions, hence various thermal sensitivity to track annealing, are present. Electron microprobe analyses performed on five ODP samples from the central part of the CIG ridge show that fluorapatites (losing tracks at about 105 °C) are predominant over chlorapatites (losing tracks at about 120 °C) (Green *et al.*, 1989). The distribution of individual grains FT ages in samples EN02-7 and EN02-8 might be a consequence of such a mixing.

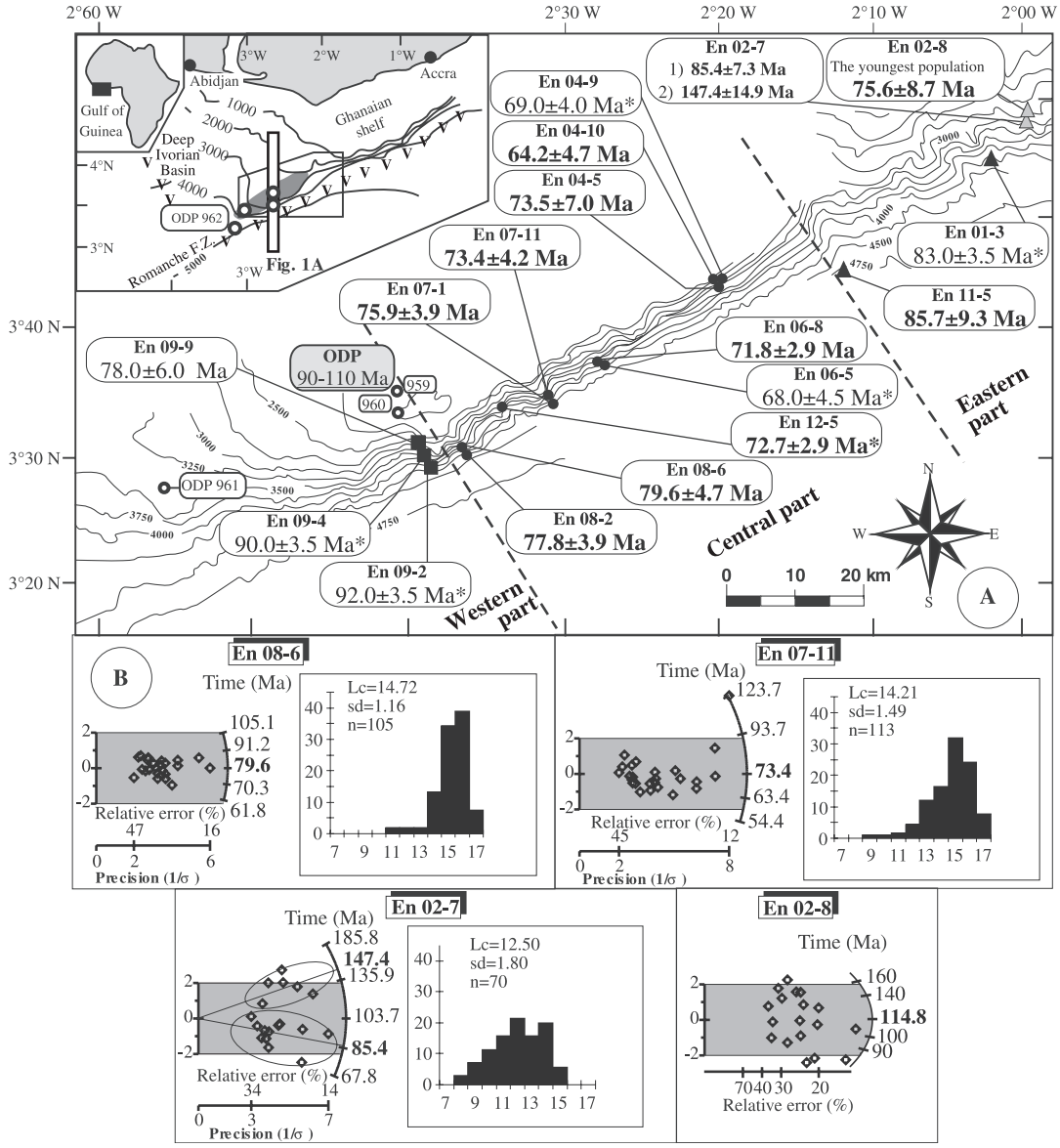

Fig. 2 Bathymetry (in m) and fission track ages of the CIG transform margin. (A) Samples from diving and ODP sites located on a bathymetric map. Insert: main morphostructural features of the CIG margin and location of Fig. 1A (V indicates the continent-ocean boundary; the CIG ridge is shaded). Main map: black triangles, circles and squares refer to eastern, central and western areas, respectively (see text) with $P(\chi^2) > 5\%$. Samples dated in this study are in bold, samples from Bouillin *et al*. (1997) are in italic, samples from ODP (studied by Bouillin *et al*., 1998 and Clift *et al*., 1998) are underlined. Asterisks indicate weighted ages. $P(\chi^2)$ computed following Green (1981). (B) Radial plots (age precision for each counted apatite grain) and confined fossil fission track length distribution in CIG samples from three different zones. Lc, SD, *n* are average length of confined fossil tracks measured, standard deviation and number of tracks, respectively.

Discussion and conclusion

Heating

Most apatites from ODP sites 959 and 960 belong to a siliciclastic sedimentary unit, respectively, early Albian (105 Ma) and late Turonian (90 Ma) in age, overlying an erosional unconformity. For these samples with central ages in the range from 90 to 110 Ma and mean confined track lengths 12.4 to 13.7 μm, modelling of FT lengths suggests a first recording of tracks at about 110–115 Ma, that means before the deposition (Bouillin *et al*., 1998; Clift *et al*., 1998). So, the post-unconformity sediments were not heated above 60 °C (Holmes, 1998; Wagner and Pletsch, 2001). Only one ODP sample retrieved from below the unconformity at site 959 shows a single population central age of 88 ± 4 Ma (Clift *et al*., 1998) indicating that all their FT were lost *in situ* by heating after their sedimentation. Similarly, detrital apatites sampled along the southern continental slope were heated after their sedimentation, and FT were lost either partially for

Table 1 Fission track analytical data

Sample W->E	Depth (m)	*n*	Df (10^5/cm^2)	Nf	Di (10^5/cm^2)	Ni	Dm (10^5/cm^2)	Nm	Dispersion (%) P(χ^2)	Dispersion (%) SE	ζ	t ± 1σ (Ma)	Lc (μm)	SD (μm)	nc
En 01-3	*−3479*	*14*	*12.5*	*(1275)*	*13.4*	*(1363)*	*5.302*	*(17910)*	*>99*	–	*339 ± 7*	*84 ± 8‡*	*14.58*	*1.22*	*52*
		10	*8.63*	*(286)*	*9.15*	*(303)*	*5.302*	*(17910)*	*>99*	–	*321 ± 4*	*80 ± 13***			
												*83.0 ± 3.5**			
En 02-8	−2800	18	16.29	(1124)	7.13	(492)	3.369	(9090)	R	R	297 ± 17	125.3 ± 10.6†	–	–	–
		5							96.9	<1		*75.6 ± 8.7*			
Young															
En 02-7	−2900	18	12.63	(1283)	5.94	(603)	3.369	(9090)	<1	21.39	297 ± 17	103.7 ± 6.9†	12.50	1.80	70
	pop. 1	12	2.58	(699)	1.50	(407)	3.369	(9090)	94.9	<1		85.4 ± 7.3			
	pop. 2	6	4.31	(584)	1.45	(196)	3.369	(9090)	74.7	<1		147.4 ± 14.9			
En 04-5	−2600	13	6.72	(597)	4.57	(406)	3.369	(9090)	22.6	13	297 ± 17	73.5 ± 7.0†	–	–	–
En 04-9	*−2405*	*17*	*4.10*	*(486)*	*3.71*	*(440)*	*3.793*	*(5017)*	*53.4*	–	*339 ± 7*	*71 ± 10‡*	*15.21*	*1.22*	*20*
		10	*4.50*	*(149)*	*4.14*	*(137)*	*3.79*	*(5017)*	*>99*	–	*321 ± 4*	*66 ± 13***			
												*69.0 ± 4.0**			
En 04-10	−2200	26	8.51	(1138)	6.60	(882)	3.369	(9090)	94.6	<1	297 ± 17	64.2 ± 4.7†	14.39	1.26	99
En 06-5	*−3465*	*8*	*6.38*	*(355)*	*5.99*	*(333)*	*3.865*	*(10223)*	*>99*	–	*339 ± 7*	*70 ± 11‡*	*14.44*	*1.21*	*45*
		25	*5.00*	*(387)*	*4.82*	*(373)*	*3.865*	*(10223)*	*>99*	–	*322 ± 25*	*65 ± 14¶*			
												*68.0 ± 4.5**			
En 06-8	−3300	33	8.63	(2024)	7.39	(1735)	3.748	(17350)	97,3	<1	330 ± 7	71.8 ± 2.9†	14.68	1.37	89
En 07-1	−4300	30	7.16	(1040)	5.98	(868)	3.862	(12259)	>99	<1	330 ± 7	75,9 ± 3.9†	–	–	–
En 07-11	−3600	25	11.43	(1273)	9.27	(1033)	3.748	(17350)	20,0	14	330 ± 7	73.4 ± 4.2†	14.21	1.49	113
En 08-2	−4400	30	8.98	(1137)	7.10	(899)	3.748	(17350)	>99	<1	330 ± 7	77.8 ± 3.9†	14.00	1.40	97
En 08-6	−3700	24	6.10	(775)	4.72	(599)	3.748	(17350)	>99	<1	330 ± 7	79.6 ± 4.7†	14.72	1.16	105
En 09-2	*−3905*	*22*	*10.01*	*(1785)*	*7.21*	*(1287)*	*3.793*	*(5017)*	*87*	–	*339 ± 7*	*89 ± 8‡*	*15.16*	*1.13*	*65*
		5	*6.59*	*(218)*	*5.05*	*(167)*	*5.302*	*(17910)*	*85.25*	–	*339 ± 7*	*117 ± 24‡*			
												*92.0 ± 3.5**			
En 09-4	*−3524*	*18*	*12.4*	*(1231)*	*8.71*	*(861)*	*3.793*	*(5017)*	*>99*	–	*339 ± 7*	*92 ± 9‡*	*14.82*	*1.15*	*74*
		14	*9.67*	*(902)*	*7.22*	*(673)*	*3.793*	*(10223)*	*>99*	–	*339 ± 7*	*88 ± 10‡*			
												*90.0 ± 3.5**			
En 09-9	*−2675*	*12*	*6.11*	*(374)*	*5.10*	*(312)*	*3.865*	*(10223)*	*>99*	–	*339 ± 7*	*78.0 ± 6.0‡*	*14.24*	*1.12*	*16*
En 11-5	−4800	5	5.59	(213)	4.02	(153)	3.862	(12259)	98.0	<1	330 ± 7	85.7 ± 9.3†	–	–	–
En 12-5	−3300	15	7.32	(904)	6.11	(755)	3.748	(17350)	90.2	<1	330 ± 7	73.7 ± 4.0†	14.22	1.29	105
		11	7.10	(733)	5.85	(604)	3.748	(17350)	>99	<1	316 ± 7	71.5 ± 4.3§			
												72.7 ± 2.9*			

Total number of tracks and track density in kapton external detectors associated with neutron glass wafer monitors NIST 962 or CN5. Each observer have a zeta (ζ) calibration factor (Fleischer and Hart, 1972).

P(χ^2), probability of χ^2 for *n* degrees of freedom where n = number of crystals dated – 1 (Galbraith, 1981; Green, 1981); R, refused test; italic characters are pooled statistics ages (Bouillin *et al.*, 1997) following Galbraith (1981) and Green (1981); normal characters are central ages calculated with their standard error (SE) (Galbraith and Laslett, 1993; Dunkl, 2001, 2002).

n, number of crystal dated; Df, Di, Dm, spontaneous, induced and monitor track densities, respectively; Nf, Ni, Nm, spontaneous, induced and monitor track counted, respectively; Lc, SD, nc, confined tracks, standard deviation and number of confined tracks measured.

*Weighted values †Florence Bigot-Cormier ‡Erika Labrin §Ali Azdimousa ¶Florence Gillot **Naima Sabil

Datations by † (for a part), §, ¶ from Bouillin *et al.* (1997).

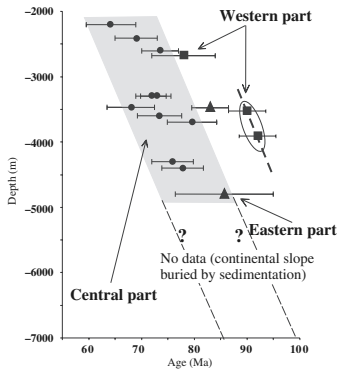

Fig. 3 Age/depth diagram. Same symbols as Fig. 2A.

samples EN02-7 and EN02-8, or completely for all other samples. So *in situ* heating of apatites reached more than 120 °C below the unconformity and all along the southern slope, except in the eastern part where the maximum temperatures reached were between approximately 105 °C and 120 °C at sites EN02-7 and EN02-8.

Heating associated to the Santonian (85–80 Ma) oceanic accretion axis cannot be responsible for the older *in situ* heating at the western end of the ridge (> 90 Ma, samples EN9-2 and EN9-4; Fig. 2A). Nevertheless, this heating mechanism cannot be excluded for the younger samples. We suggest as an alternative mechanism that heating was associated to sedimentary burial, probably with an high geothermal gradient (present-day gradient 48 °C km^{-1} at ODP site 959; Mascle *et al.*, 1996) during deposition of the very thick Aptian–Albian sedimentary unit in intracontinental transform basins (Basile *et al.*, 1998).

Cooling and denudation

All samples with a single grain age population (P(χ^2) > 5%) are represented in the age/depth diagram of Fig. 3.

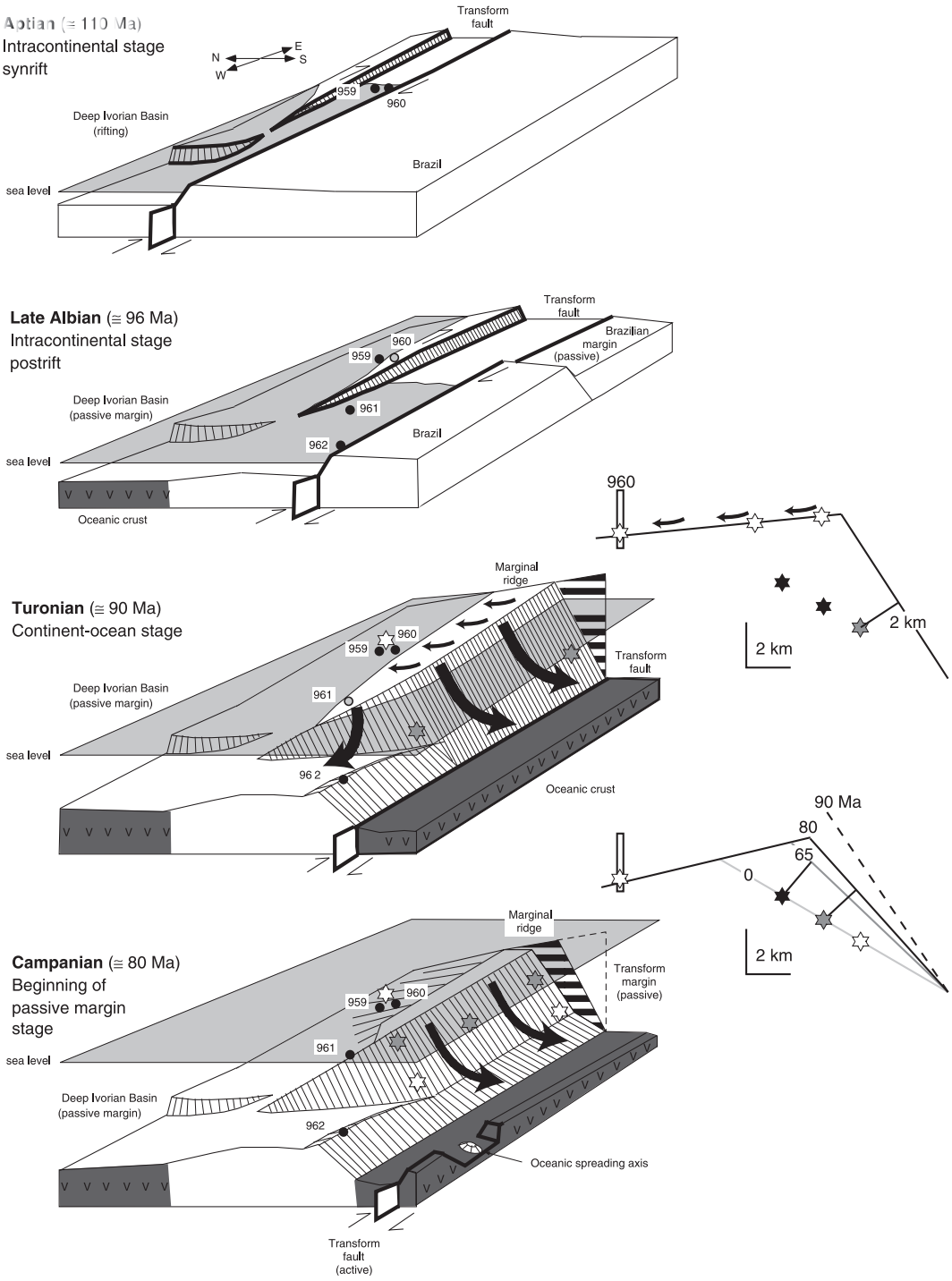

Fig. 4 Evolution of the CIG margin (modified from Basile *et al.*, 1998) with location of ODP sites 959 to 962 (black dots when below sea level, grey dots above sea level). Sediments overlying the continental unconformity surface (from Late Albian stage to present-day) and the oceanic crust are not shown. Approximate scales 110 km horizontally along transform fault, and 7 km vertically between the top of the marginal ridge and the adjacent oceanic crust (Campanian stage). To the right, zoom on a section of the marginal ridge (without vertical exaggeration) with the expected position of the continental slope at 90, 80, 65 Ma and present day (0). At each stage the 120 °C isotherm is assumed to be parallel to the sea floor at 2 km depth. See text for further comments. Black stars, samples hotter than 120 °C; grey stars, samples cooling from 120 to 60 °C; white stars, samples previously cooled; banded section represents the part of the continental slope eroded from the previous stage; large arrows indicate the erosion of the marginal ridge and transport of detrital sediments. Bold lines indicate active faults.

There is a clear age/depth correlation, with the older ages systematically at the bottom of the continental slope, and the younger ages at the top, unlike what is commonly observed in continental areas. Moreover, clear-cut correlations appear in each of the three morpho-structural units (western, central and eastern) of the continental slope. In each area, denudation and cooling started in the vicinity of the continental slope bottom and reached its top (2 km higher) 10 Myr later. This striking result can be explained by retrogressive erosion of the continental slope: if the bottom of the continental slope was fixed while its steepness decreased with time, the cooling of samples distributed across today's slope occurred later at the top than at the bottom (sections in Fig. 4).

In this retrogressive mechanism, the FT ages from the sediments overlying the unconformity on the northern slope of the ridge (90–110 Ma, see Bouillin *et al*., 1998 and Clift *et al*., 1998) result from previously cooled apatites, all older than the erosion phase recorded by the unconformity, eroded near the crest of the marginal ridge and transported along the northern slope (Fig. 4). On the contrary, the apatites on the southern slope are cooled *in situ* as soon as they are close enough to the surface, since the formation of the continental slope at the very bottom (now covered by a thick sedimentary pile), and more and more recently towards the crest of the ridge as soon as the continental slope steps backwards, probably by gravity sliding on a very steep slope (Fig. 4). Before the oceanic accretion against the transform margin, the sediments produced by the erosion of the continental slope were transported on the oceanic crust, and now lie in the Romanche Fracture Zone several thousand kilometres west of the CIG margin (Honnorez *et al*., 1993; Bonatti *et al*., 1996). After the oceanic accretion, erosion of the continental slope resulted in very thick sedimentary units (more than 2 km; Fig. 1) overlying the new crust.

To explain previously published cooling ages, Clift and Lorenzo (1999) proposed a transtensional tectonic unloading this margin. Nevertheless, there is not very clear structural argument neither in seismic data nor in the scarp to support this hypothesis. Moreover, denudation by a transtensional fault located along the continental slope may produce older FT ages at the top of the slope than at the bottom. The new set of FT data presented in this paper clearly discard Clift and Lorenzo (1999) hypothesis, and makes the proposed retrogressive erosion much more reasonable.

Seismic sections show that the base of the continental slope is between 6 and 7 km deep (Fig. 1; Sage *et al*., 1997). An extrapolation of the age/depth correlation to such depths indicates that denudation might have started *c*. 90 Ma in the eastern and central parts of the continental slope, and >100 Ma in the western part (Fig. 3). These ages are consistent with the formation of a late Albian deep basin west of the marginal ridge (ODP site 962, Basile *et al*., 1998), and with a deep transform valley bounding the continental slope during the Turonian continent-ocean active transform stage (Fig. 4). Consequently, the overall thermal history/denudation of this margin seems to be associated with this active transform stage, and not as previously expected to the passing of the oceanic accretion axis. In all areas, cooling at the top of the continental slope seems to be contemporaneous and younger than 80 Ma, with the partial exception of the easternmost samples that where not buried enough to erase the previous FT.

Finally, the retrogressive erosion which affected the marginal ridge produced an important lithospheric discharge, that increased both with the deepening of the crust sliding against the transform margin (from thick continental crust to thin continental crust, and finally to oceanic crust; Fig. 4) and with the retrogressive erosion, and that might have initiated the flexural uplift of the CIG ridge (Basile and Allemand, 2002).

Acknowledgement

We wish to thank the Equanaute crew and more specially J. Mascle, M. Guiraud, J. Benkhelil, G. Mascle and M. Cousin, scientists who sampled the CIG ridge from the Nautile. We also thank three anonymous reviewers for their fruitful comments. This article is Geosciences Azur contribution number 701.

References

Basile, C. and Allemand, P., 2002. Erosion and flexural uplift along transform faults. *Geophys. J. Int*., **151**, 646–653.

Basile, C., Mascle, J., Popoff, M., Bouillin, J.-P. and Mascle, G., 1993. The Côte d'Ivoire-Ghana transform margin: a marginal ridge structure deduced from seismic data. *Tectonophysics*, **222**, 1–19.

Basile, C., Mascle, J., Benkhelil, J. and Bouillin, J.-P., 1998. Geodynamic evolution of the Cote d'Ivoire-Ghana transform margin; an overview of Leg 159 results. *Proc. ODP Sci. Results*, **159**, 101–110.

Blarez, E. and Mascle, J., 1988. Shallow structure and evolution of the ivory coast and Ghana transform margin. *Mar. Petrol. Geol*., **5**, 54–64.

Bonatti, E., Ligi, M., Borsetti, A.M., Gasperini, L., Negri, A. and Sartori, R., 1996. Lower Cretaceous deposits trapped near the equatorial Mid-Atlantic Ridge. *Nature*, **380**, 6574, 518–520.

Bouillin, J.P., Poupeau, G., Riou, L., Sabil, E., Basile, C., Mascle, J., Mascle, G. and the Equanaute Group, 1994. La marge transformante de Côte d'Ivoire-Ghana: premières données thermochronologiques (campagne Equanaute, 1992). *CR Acad. Sci. Paris*, **318**, 1365–1370.

Bouillin, J.-P., Poupeau, G., Labrin, E., Basile, C., Sabil, N., Mascle, J., Mascle, G., Guillot, F. and Riou, L., 1997. Fission track study: heating and denudation of marginal ridge of the Ivory Coast-Ghana transform margin. *Geo-Mar. Lett*., **17**, 55–61.

Bouillin, J.-P., Poupeau, G., Basile, C., Labrin, E. and Mascle, J., 1998. Thermal constraints on the Côte d'Ivoire-Ghana transform margin: evidence from apatite fission tracks. *Proc. ODP Sci. Results*, **159**, 43–48.

Clift, P.D. and Lorenzo, J.M., 1999. Flexural unloading and uplift along the Côte d'Ivoire-Ghana transform margin, equatorial Atlantic. *J. Geophys. Res*., **104**, B11, 25257–25274.

Clift, P.D., Carter, A. and Hurford, A.J., 1998. Apatite fission track dating of ODP sites 959 and 960 on the transform continental margin of Ghana, west Africa. *Proc. ODP Sci. Results*, **159**, 35–41.

Dunkl, I., 2001. The additional parameters - a short introduction to the data handling with TRACKKEY 4.1. *OnTrack*, **11**, 19–22.

Dunkl, I., 2002. TRACKKEY: a Windows program for calculation and graphical presentation of fission track data. *Comput. Geosci*., **28**, 3–12.

Fleischer, R.L., Hart, H.R. Jr, 1972. Fission track dating: techniques and problems. In: *Calibration of Hominoid*

Evolution (W.W. Bishop, J.A. Miller and S. Cole, eds), pp. 135–170. Scottish Academic Press, Edinburgh.

Galbraith, R., 1981. On stastitical models for fission track counts. *Math. Geol.*, **13**, 471–488.

Galbraith, R.F. and Laslett, G.M., 1993. Statistical models for mixed fission track ages. *Nucl. Tracks Radiat. Meas.*, **21**, 459–470.

Green, P.F., 1981. A new look at stastistics in fission tracks dating. *Nucl. Tracks*, **5**, 76–86.

Green, P.F., Duddy, I.R., Gleadow, A.J.W. and Lovering, J.F., 1989. Apatite fission track analysis as a paleotemperature indicator for hydrocarbon exploration. In: *Thermal History of Sedimentary Basins* (N.D. Neaser and T.H. McCullogh, eds), pp. 1–2. Springer Verlag, New York.

Holmes, M.A., 1998. Thermal diagenesis of Cretaceous sediment recovered at the Côte d'Ivoire-Ghana transform margin. In: *Proceedings of the Ocean Drilling Program, Scientific Results*, **Vol. 159** (J. Mascle, G.P. Lohmann and P.D. Clift, eds), 53–70.

Honnorez, J., Villeneuve, M. and Mascle, J., 1993. Old continent-derived metasedimentary rocks in the equatorial atlantic – an acoustic basement outcrop along the fossil trace of the Romanche Transform Fault at 6 degrees 30′W. *Mar. Geol.*, **117**, 1–4, 237–251.

Hurford, A.J. and Carter, A.J.W., 1991. The role of fission track dating in discrimination of provenance. In: *Developments in Sedimentary Provenance Studies, PDW Haughton* (A.C. Morton and S.P. Todd, eds), *Geol. Soc. Lond. Spec. Publ.*, **57**, 67–78.

Hurford, A.J. and Green, P.F., 1983. The zeta calibration of fission track dating. *Isot. Geosci.*, **1**, 285–317.

Klingebiel, A., 1976. Sediments et milieux sedimentaires dans le golfe de Benin. Bulletin du Centre de Recherche Exploration. Production. Elf Aquitaine, **Vol. 1**, 129–148.

Lamarche, G., Basile, C., Mascle, J. and Sage F., 1997. The Côte d'Ivoire - Ghana transform margin: sedimentary and tectonic structure from MCS data. *Geo-Mar. Lett.*, **17**, 62–69.

Mascle, J. and Basile, C., 1998. Marges continentales transformantes. *CR. Acad. Sci. Paris*, **326**, 827–838.

Mascle, J. and Blarez, E., 1987. Evidence for transform margin evolution from the Ivory Coast-Ghana continental margin. *Nature*, **326**, 378–381.

Mascle, J., Blarez, E. and Marinho, M., 1988. The shallow structure of the Guinea and Côte d'Ivoire-Ghana transform margins: their bearing on the equatorial atlantic mesozoic evolution. *Tectonophysics*, **155**, 193–209.

Mascle, J., Lohmann, G.P., Clift, P.D. and shipboard scientific party, 1996. *Proceedings of the Ocean Drilling Program, Scientific Results*, Vol. 159, 616 pp.

Mascle, J., Guiraud, M., Benkhelil, J., Basile, C., Bouillin, J.-P., Mascle, G., Cousin, M., Durand, M., Dejax, J. and Moullade, M., 1998. A geological field trip to the Côte d'Ivoire-Ghana transform margin. *Oceanolog. Acta*, **21**, 1–20.

Sage, F., Pontoise, B., Mascle, J., Basile, C. and Arnould, L., 1997. Crustal structure and ocean-continent transition at marginal ridge: the Côte d'Ivoire-Ghana marginal ridge. *Geo-Mar. Lett.*, **17**, 40–48.

Sage, F., Basile, Ch., Mascle, J., Pontoise, B. and Whitmarsh R.B., 2000. Crustal structure of the continent-ocean transition off the Côte d'Ivoire-Ghana transform margin: implications for thermal exchanges across the palaeotransform boundary. *Geophys. J. Int.*, **143**, 662–678.

Todd, B.J. and Keen, C.E., 1989. Temperature effects and their geological consequences at transform margins. *Can. J. Earth Sci.*, **26**, 2591–2603.

Wagner, T. and Pletsch, T., 2001. No major thermal event on the mid-Cretaceous Côte d'Ivoire-Ghana transform margin. *Terra Nova*, **13**, 165–171.

Received 20 April 2004; revised version accepted 10 January 2005

